Mechanical Properties of the Sarcolemma and Myoplasm in Frog Muscle as a Function of Sarcomere Length

STANLEY I. RAPOPORT

From the Laboratory of Neurophysiology, National Institute of Mental Health, Bethesda, Maryland 20014

ABSTRACT The elastimeter method was applied to the single muscle fiber of the frog semitendinosus to obtain the elastic moduli of the sarcolemma and myoplasm, as well as their relative contributions to resting fiber tension at different extensions. A bleb which was sucked into a flat-mouthed pipette at the fiber surface separated into an external sarcolemmal membrane and a thick inner myoplasmic region. Measurements showed that the sarcolemma does not contribute to intact fiber tension at sarcomere lengths below 3 μ. It was estimated that the sarcolemma contributed on the order of 10% to intact fiber tension at sarcomere lengths between 3 and 3.75 μ, and more so with further extension. Between these sarcomere lengths, the sarcolemma can be linearly extended and has a longitudinal elastic modulus of 5×10^6 dyne/cm^2 (assuming a thickness of 0.1 μ). Resistance to deformation of the inner bleb region is due to myoplasmic elasticity. The myoplasmic elastic modulus was estimated by use of a model and was used to predict a fiber length-tension curve which agreed approximately with observations.

INTRODUCTION

Knowledge of the relative contributions of sarcolemma and myoplasm to resting muscle tension is important to the understanding of muscle function. Correct estimates of myofilamentary resting tension at different degrees of overlap of actin and myosin filaments would help to show whether tension arises from interfilamentary interaction, as in contraction (Hill, 1968), or from other sources. Although the sarcolemma when extended can exert tension equal to whole fiber tension (Street and Ramsey, 1965), its exact contribution to passive tension at different fiber extensions is not certain.

Experiments on the myofibrillar preparation in oil indicate that the sarcolemma contributes 80% of passive fiber tension at sarcomere lengths (S.L.) above 3.2 μ (Podolsky, 1964). On the other hand, experiments with the tubular sarcolemmal preparation indicate that the sarcolemmal contribution is

<50% even to extensions twice fiber rest length (Casella, 1950). Conclusions based on the tubular preparation, however, are open to reservations. The sarcolemmal tube is formed by damaging a single fiber so as to produce a sarcolemmal region free of myoplasm, and may differ structurally from the sarcolemma in the intact fiber. Furthermore, the rest length of the tubular sarcolemma cannot be referred accurately to sarcolemmal rest length in the intact fiber (see Casella, 1950; Rapoport and FitzHugh, 1971).

I used the elastimeter method, described by Mitchison and Swann (1954) and Rand and Burton (1964), to obtain the sarcolemmal contribution to fiber tension in a way which partially meets these objections. A bleb on the surface of a single muscle fiber is sucked into a flat-mouthed pipette and its vertical displacement is measured at different suction pressures. At high pressures, an external membrane M_o, which probably consists of the outer three layers of the sarcolemma, separates from the inner myoplasmic region R_i without producing a contracture. The pressure-displacement relation of the bleb surface then shows hysteresis; its return leg permits calculation of tension of M_o which, when subtracted from the rising leg of the hysteresis curve, gives the mechanical properties of R_i.

The fiber is undamaged by the elastimeter method, and M_o (presumably the sarcolemma) may be closer to its natural condition than in the tubular preparation. In addition, rest lengths of M_o and R_i can be referred accurately to fiber sarcomere length and the correctly referred elastic moduli can be used to understand the components of whole fiber elasticity. A preliminary report of this work has been published (Rapoport, 1970).

LIST OF SYMBOLS

c diameter of pipette = base of bleb (Fig. 5)

d fiber diameter; at S.L. = 2 μ, $d = d_2$

e extension; at reference S.L. = 2 μ, $e = e_2$; at reference S.L. = 3 μ, $e = e_3$ (equation 5)

E elastic modulus, dyne/cm^2 (equation 11)

$E(y)$ elastic modulus in bleb at $y \geq 0$ (Fig. 16)

f correction factor in calculating stretch (equation 2, Fig. 5)

g estimated depth below fiber surface to which tension lines are displaced

h vertical displacement of bleb

M_o outer membrane which separates from bleb

o, i subscripts which designate outer membrane and inner region of bleb, respectively

P suction pressure in pipette, dyne/cm^2

r radius of curvature of spherical bleb surface

r_1, r_2 radii of curvature normal to each other of a curved surface (equation 6)

R_i inner region of bleb

s length of bleb arc

S.L. sarcomere length, μ

$x(y)$ vertical displacement of tension lines in bleb

$\gamma_{\text{longitudinal, }o}$ tension of M_o directed parallel to the fiber axis, dyne/cm

$\gamma_{circumferential,\ o}$ tension of M_o directed normal to the fiber axis (in transverse plane), dyne/cm

γ_o elastic tension of membrane M_o, dyne/cm (equation 7)

γ_{i+o} equivalent combined tension of $M_o + R_i$, dyne/cm (equation 9)

γ_1, γ_2 surface tensions normal to each other of a curved surface, dyne/cm (equation 6)

METHODS

A semitendinosus fiber of *Rana pipiens* was dissected from the whole muscle and mounted at room temperature (about 22°C) in the chamber of Fig. 1 *a*, which was placed on a microscope stage. The fiber was photographed using a water immersion objective (E. Leitz, Inc., Rockleigh, N. J.; U − O, 75 w, A = 0.90) and × 5 eyepiece. One end was fixed in position and the other moved to stretch the fiber.

The fiber was stimulated two to three times to test whether it gave an observable twitch along its length, and to eliminate aftereffects of stretching during manipulation (Buchthal et al., 1951, p. 40). A flat-mouthed pipette, prepared by the method of Fonbrune (1949), was placed with a micromanipulator against a surface region

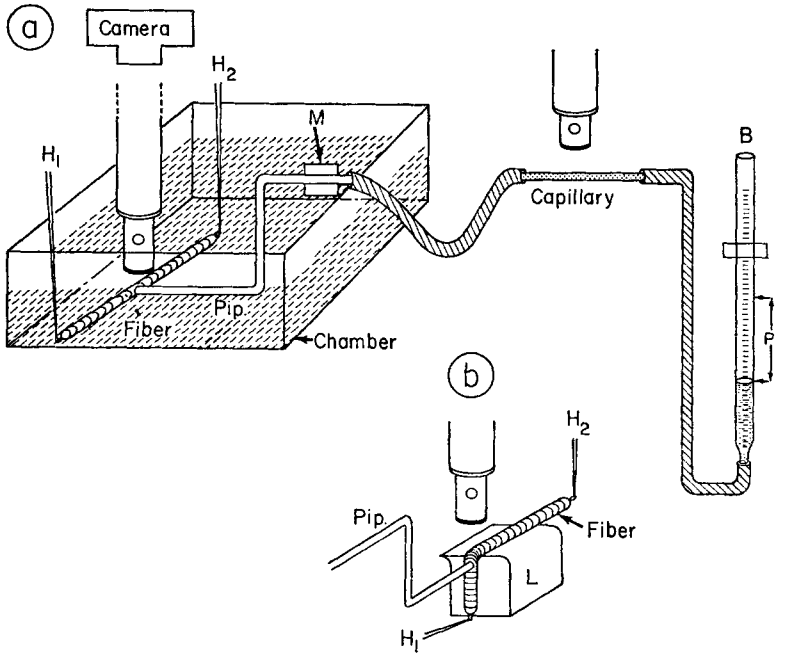

FIGURE 1. Experimental arrangement. Fig. 1 *a*, measurement of bleb in longitudinal plane of fiber. The fiber is held fixed by holder (H_2) and moved by holder (H_1). The bleb is observed and photographed through the objective (O) of the microscope. The pipette (*Pip.*) is placed against the fiber by the micromanipulator (M), connected to the capillary in which fat droplets show direction of movement; the burette is (B); height can be varied to control suction pressure (P). Fig. 1 *b*, measurement of bleb in transverse plane of fiber. The fiber is bent over the Lucite block (L) with a lip. The microscope is focused on a region of bleb (see Fig. 4).

apparently free of connective tissue. In some cases the fiber was bent at right angles and the pipette placed as shown in Fig. 1 *b* to obtain a picture in the transverse plane of the fiber. The inner pipette diameter was between 29 and 37 μ, less than or equal to about one-half a fiber diameter. The pipette was connected by a 2 mm in diameter glass capillary to a burette whose fluid height could be regulated and read to ± 0.2 mm. The system was filled with the solution bathing the fiber. Microscopic movements of cream fat droplets placed in the connecting capillary showed the presence and direction of volume flow. Fluid height in the burette was adjusted first to obtain zero flow (this is the baseline height and the same as the height of the fluid level in the chamber), and then reduced to obtain a suction pressure P at the mouth of the pipette, which was then pressed against the fiber. Absence of fat droplet movement indicated a good seal, after which a series of measurements and photographs was made with progressively increasing and then decreasing suction pressures (Figs. 2–4).

Displacement following a pressure step stabilized in <4 min, but each measurement was obtained after about 10 min. Pressure-vertical displacement curves were obtained on one fiber at different regions as a function of sarcomere length, which was calculated by comparing photographs of the fiber and of an immersed micrometer scale. 62 regions were studied in 22 fibers. After a region was analyzed, the fiber was stimulated to see whether a sharp twitch was observed along its length. If not, or if a contracture clot which had not been induced purposely had formed, the earlier measurements were rejected.

Experiments were done in isotonic Ringer and in 75 and 50% hypotonic Ringer, the compositions of which are given in Table I. The results in the hypotonic solutions did not differ from each other and were lumped together under the title "hypotonic Ringer."

In some cases, the tightness of the seal was tested by measuring electrical resistance at the pipette mouth after a bleb was formed. Current first was passed through the unattached pipette and through the balanced bridge circuit of a Bak Amplifier (ELSA 4). Then the pipette was placed against the fiber and the bleb sucked in. For example, the measured additional resistance was 0.3 MΩ for a pipette with a diameter of 36 μ. Since the resistance of the fiber membrane is about 2000 ohm cm^2 (Fatt, 1964), the 0.3 MΩ was due to leakage between the pipette inner surface and the external solution. The specific resistance of Ringer is about 100 ohm cm^2 (Fatt, 1964). Taking the length of adhesion of the bleb to the pipette wall to be between 1 and 5 μ, the thickness of the region between the bleb and pipette was estimated to be between 0.15 and 0.03 μ. This equivalent thickness could be due to the resistivity of the outer reticular and collagen layers of the sarcolemma (Mauro and Adams, 1961).

Treatment of Data The bleb which was sucked into the pipette approximates a spherical arc the radius of curvature r of which is (Dull, 1941):

$$r = c^2/8h + h/2 \qquad (1)$$

where c is pipette diameter and h is vertical displacement of the bleb surface. If the surface is stretched without new material being drawn into the pipette, then the sarcomere length (S.L.) at the bleb surface increases, and the S.L. at the pipette

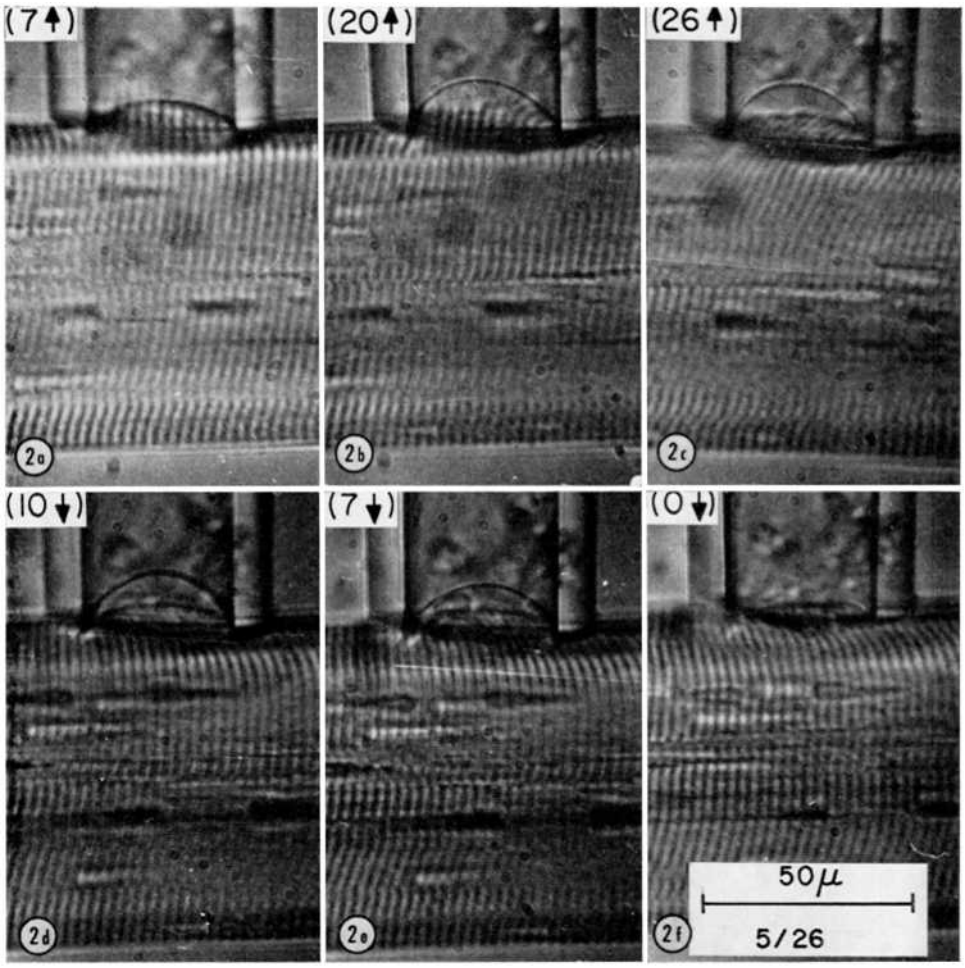

FIGURE 2. Formation of bleb at a fiber region and separation of M_o with increasing and decreasing suction pressure; hypotonic Ringer. S.L. = 2.89 μ, c = 34.6 μ. P in dyne/cm^2 $\times$ 10^3 is given in the left upper corner of each figure. Arrows indicate if pressure is increasing or decreasing in hysteresis analysis. M_o has separated from R_i in (*c*), remains separated in (*e*), even though P is the same as in (*a*), and reattaches to R_i in (*f*).

mouth remains equal to the S.L. in the fiber body (Fig. 5 *a*). If an adjacent region is drawn into the pipette, the S.L. at the mouth decreases (Fig. 5 *b*). We can use the relative sarcomere lengths at the fiber body and at the pipette mouth to estimate the extra membrane, if any, that is drawn into the pipette. The ratio f is defined as

$$f = \frac{\text{S.L. in body}}{\text{S.L. at mouth}} = \frac{\text{sarcomeres/cm at mouth}}{\text{sarcomeres/cm in body}} \geq 1 . \qquad (2)$$

f is used to calculate the correct extension e of the bleb surface,

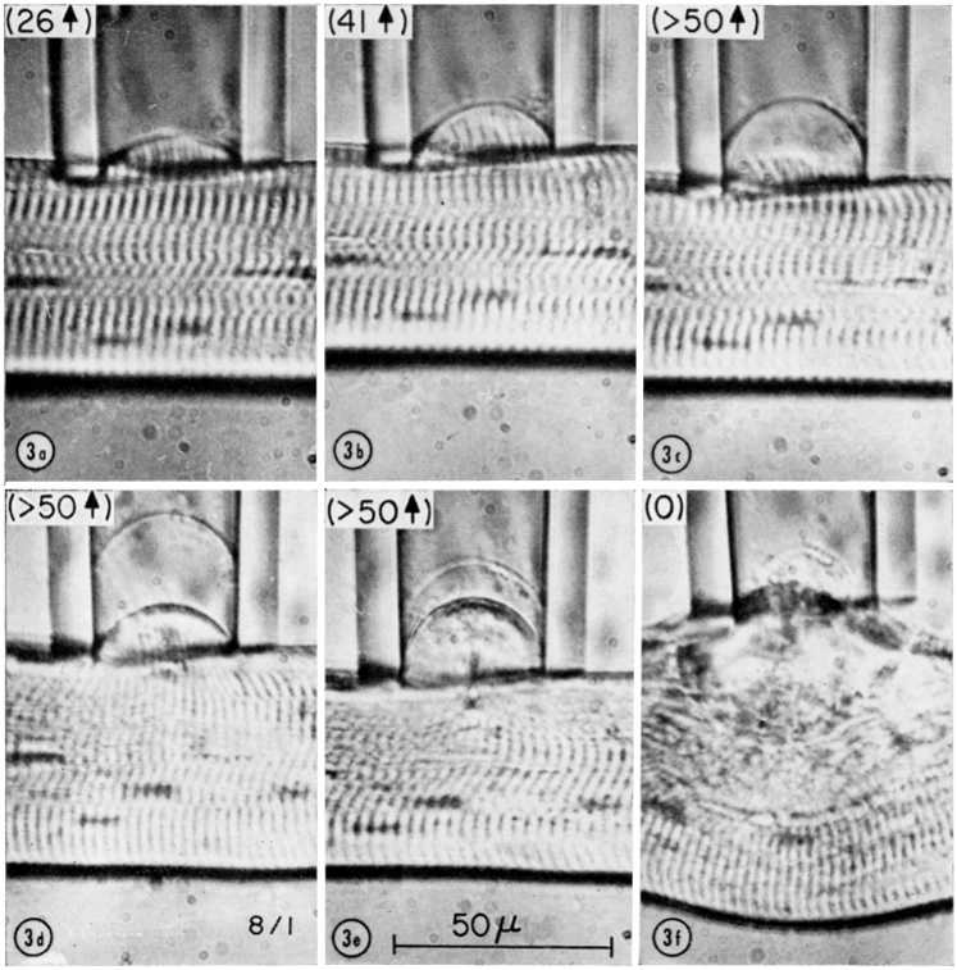

FIGURE 3. Formation of bleb at a fiber region, separation of membrane M_o, and formation of contracture clot with increasing suction pressure; Ringer. S.L. = 3.4 μ, c = 32.8 μ. P in dyne/cm^2 $\times$ 10^3 is given in left upper corners. Arrows indicate if pressure is increasing or decreasing in hysteresis plot. The figure shows spreading of sarcomeres of the bleb in (*a*) and (*b*), which were photographed 10 min apart. The pressures in (*c*)–(*e*) were adjusted by a vacuum attached to the burette in Fig. 1 *a* and were measured with a mercury manometer. (*c*) was photographed 3 min after the pressure was increased, (*d*) 3.5 min later, and (*e*), 4 min after that. (*f*) was photographed 15 sec after the pipette was released. Times shorter than 10 min were chosen because the appearance of the bleb changed continuously (see Results).

$$e = \frac{s - fc}{fc}, \tag{3}$$

where s is the length of the bleb arc (Dull, 1941),

$$s = 2r \sin^{-1}(c/2r). \tag{4}$$

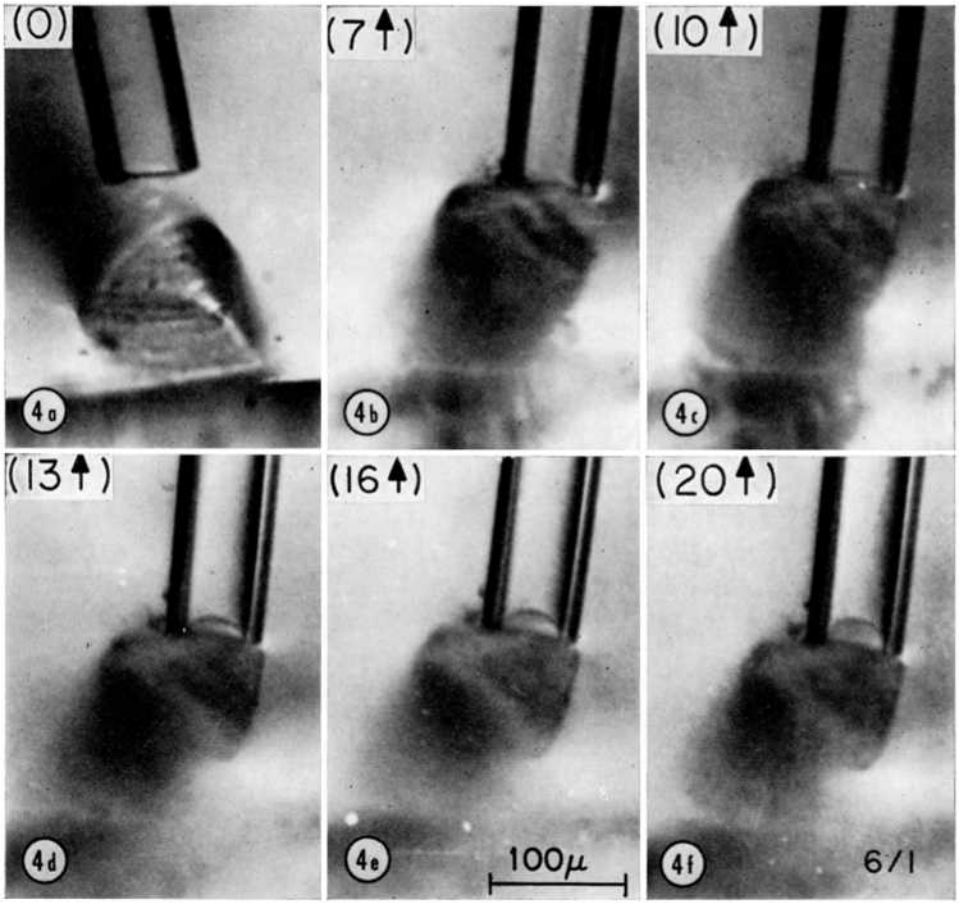

FIGURE 4. Formation of bleb at a fiber region as shown in transverse plane of fiber; Ringer. $c = 30.6\ \mu$. P in dyne/cm^2 $\times$ 10^3 is given in left upper corners. Arrows indicate if suction pressure is increasing or decreasing in hysteresis plot. The lower region in each photograph is the edge of the Lucite block. The microscope is focused at the level of bleb formation. The figure shows that the bleb surface is spherical in the transverse fiber plane.

In some cases, especially after the membrane M_o separated from R_i (see below), M_o adhered to the inner surface of the pipette some microns above the mouth (Figs. 2–4, 12). Stretch and curvature were recalculated taking this adhered region into account.

When data are referred to a reference S.L. $= 2\ \mu$, below which isolated myofibrils do not exert resting longitudinal tension (Podolsky, 1964), extension will be designated as e_2,

$$e_2 = (\text{S.L.} - 2\ \mu)/2\ \mu. \tag{5}$$

It will be shown also that M_o does not exert tension at S.L. $< 3\ \mu$; in this case, e_3 will refer to a resting S.L. of $3\ \mu$ and $e_3 = 0$ when S.L. $= 3\ \mu$. e, e_2, and e_3 are linearly related (see equations 1 *a* and 2 *a* and Fig. 8).

TABLE I
COMPOSITION OF SOLUTIONS

Solution	K^+	Na^+	Ca^{2}	Cl^-	HPO_4^{2-}	$H_2PO_4^-$	Relative tonicity*
Ringer, *mM*	2.5	120.0	1.8	121.0	2.15	0.85	1
75% hypotonic Ringer, *mM*	2.5	90.6	1.8	92.3	1.88	0.74	0.76
50% hypotonic Ringer, *mM*	2.5	61.3	1.8	63.5	1.61	0.64	0.53

* Measured by freezing point depression.

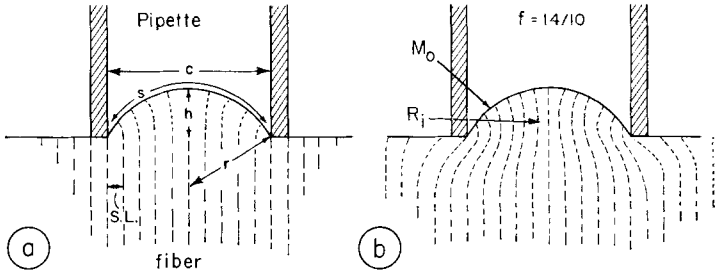

FIGURE 5. Diagram of bleb. M_o is outer membrane, R_i is inner region. r = radius of curvature of spherical arc, c = pipette inner diameter, s = length of bleb arc, h = vertical displacement. (*a*) shows that the surface has stretched because sarcomere length has increased there compared to the body of the fiber. (*b*) shows that part of the adjacent region has been drawn into the bleb, and should be compared with Fig. 12 *c* and *d*. The ratio f is given by equation 2.

RESULTS

Assumptions

Data were analyzed using the following assumptions.

(*a*) The surface of the bleb is spherical. The bleb is composed of a thin outer membrane M_o and a thick inner region R_i.

(*b*) The pressure drop across M_o, when detached from R_i, is less than or equal to the suction pressure P in the pipette (see equation 8 and Discussion).

(*c*) At mechanical equilibrium of the intact bleb, suction pressure P is balanced by the additive elastic properties of M_o and R_i. The Laplace equation for an anisotropic curved surface relates the inwardly directed pressure (which equals the pressure drop across the surface) to the surface tensions, γ_1 and γ_2 dyne/cm, and to their radii of curvature, r_1 and r_2, where the subscripts represent normal planes (Joos, 1958):

$$\text{inward pressure} = \frac{\gamma_1}{r_1} + \frac{\gamma_2}{r_2} \text{ dyne/cm}^2. \qquad (6)$$

(The γ's will increase with extension in elastic membranes but are constant for soap bubble membranes. M_o and R_i are elastic.)

If γ_1 and γ_2 are equated with the longitudinal and circumferential tensions of M_o, $\gamma_{\text{longitudinal},o}$ and $\gamma_{\text{circumferential},o}$, then a "combined" tension of M_o is defined by

$$\gamma_o = \gamma_{\text{longitudinal},o} + \gamma_{\text{circumferential},o} \text{ dyne/cm.} \tag{7}$$

When M_o has separated from R_i, the spherical surface of M_o has a single radius of curvature $r = r_1 = r_2$. From equations 6 and 7, and by assumption (*b*),

$$\gamma_o/r \leq P. \tag{8}$$

In order to compare observations on the intact bleb (R_i and M_o attached) with those on M_o when it has separated, we define an "equivalent" tension, γ_{i+o} dyne/cm, which would arise if the intact bleb were a simplified surface composed of two thin attached membranes "equivalent" to $M_o + R_i$. From equation 6, for the intact bleb

$$P = \gamma_{i+o}/r \text{ dyne/cm}^2. \tag{9}$$

P in equation 9 is the suction pressure on the intact bleb, and subtraction from it of the contribution of M_o, γ_o/r, gives the calculated contribution of R_i,

$$P - \gamma_o/r = (\gamma_{i+o} - \gamma_o)/r \text{ dyne/cm}^2. \tag{10}$$

Equation 10 can be evaluated by the model in the Appendix.

(*d*) Internal hydrostatic pressure of the muscle fiber can be neglected.

Experimental

Fig. 6 relates vertical bleb displacement h to suction pressure P for one fiber. For small displacements, hysteresis is absent when P is reduced, but at larger displacements a membrane M_o separates from the rest of the bleb R_i and then reduction of P produces hysteresis in the h–P curve. Separation of M_o from R_i occurs more readily in stretched fibers.

Fig. 7 represents a series of experiments on another fiber in which suction pressure P was raised until M_o separated from R_i, and then was reduced, at different fiber sarcomere lengths and pipette diameters. The return curves have larger displacements (h) for a given P than do the rising curves. Each return curve was divided arbitrarily into an elastic region, in which h obviously increased with P, and a more inelastic region, in which h remained approximately constant with increasing P. For instance, for S.L. = 3.38 μ in Fig. 7, the open triangles when $P > 25 \times 10^3$ dyne/cm^2 were called inelastic, and when $P < 25 \times 10^3$ dyne/cm^2 they were called elastic.

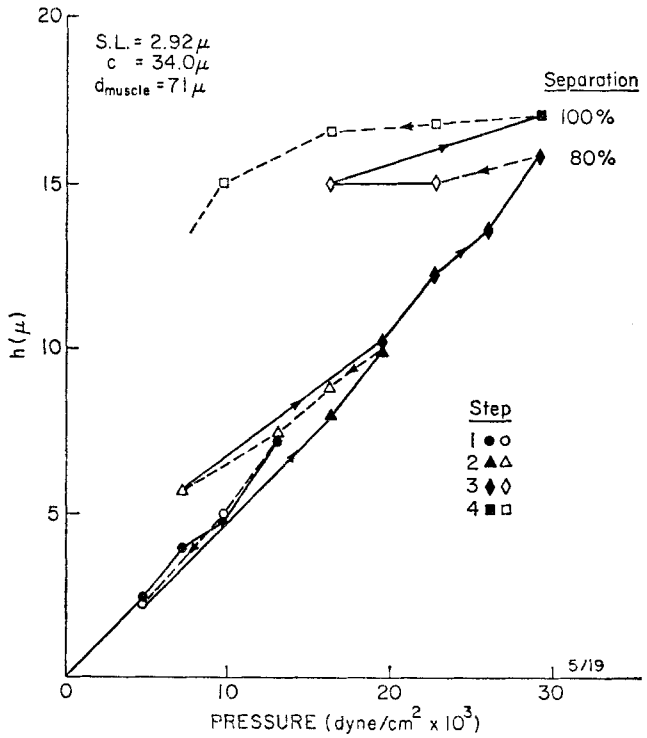

FIGURE 6. Displacement-pressure curve for one region showing development of hysteresis at large extension when separation of M_o is produced. The pressure is increased in steps (continuous lines) and then partly decreased (dashed lines). Hysteresis is evident in the displacement h after R_i has partially or completely separated from M_o.

The tensions γ_o and γ_{i+o} in Ringer, hypotonic Ringer, and return Ringer solutions were obtained by equations 1–9 from the displacement-suction pressure relations and initial sarcomere lengths (S.L.) of each bleb (Figs. 8–10). γ_{i+o} was calculated from P on the intact bleb by equation 9. γ_o was calculated from suction pressure on blebs once M_o and R_i had separated, assuming equality between P and γ_o/r in equation 8. It therefore is a calculated upper bound.

Regression lines in Figs. 8–10 were found by least squares for observations on blebs in the elastic region (filled symbols), as defined above in the discussion of Fig. 7. The open symbols represent observations in the "inelastic" regions. The SD of an observation in Figs. 8–10 was between 5.1 and 7.6 dyne/cm² for the elastic region.

In Ringer solution (Fig. 8), the regression line of γ_{i+o} intersects the abscissa at S.L. = 2.06 μ (e_2 = 0.03), with a maximum 95% confidence interval of S.L. = 1.4–2.7 μ (Brownlee, 1965). This agrees with evidence that the minimal sarcomere length of the unstretched fiber is at S.L. $\leq$ 2 μ (Podolsky,

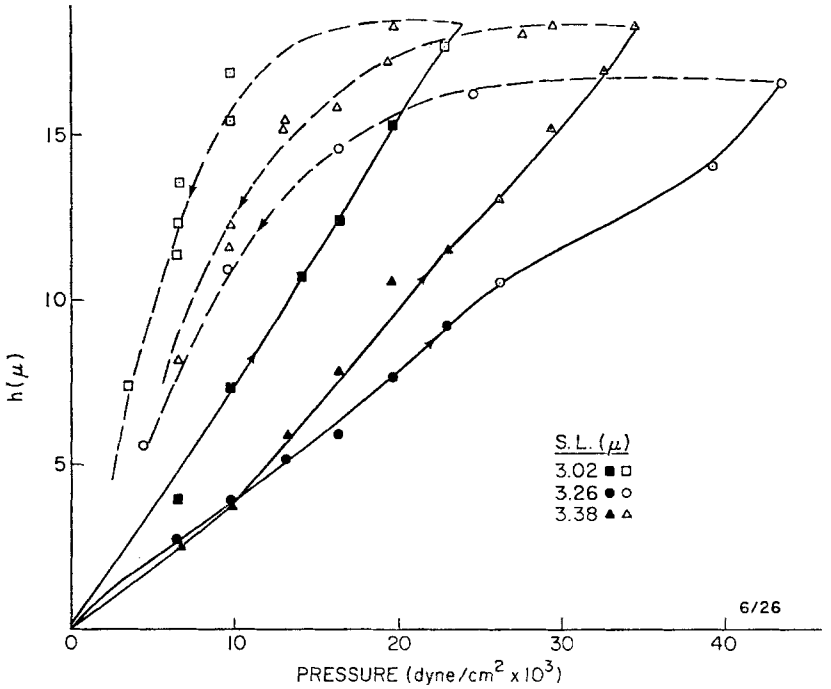

FIGURE 7. Displacement-pressure curve for three regions at different sarcomere lengths on a fiber; Ringer. For S.L. = 3.02 and 3.26 μ, c = 34.7 μ; for S.L. = 3.38 μ, c = 36.4 μ. Symbols with dots represent partial separation of M_o from R_i, filled symbols no separation, open symbols complete separation. The curves show hysteresis due to separation.

1964; Gonzalez-Serratos, 1966), and is the reason for taking e_2 as the reference extension of the intact bleb.

The tension γ_o of the outer membrane M_o becomes 0 at S.L. = 2.95 μ ($e_3 = -0.02$), with a maximum 95% confidence interval of S.L. = 2.1–3.7 μ. e_3 was therefore chosen as the reference extension of M_o.

The slope of γ_{i+o} against S.L. or e_2 is reduced significantly in hypotonic Ringer ($P < 0.05$) as illustrated by comparing Figs. 8 and 9. The slopes of the γ_o do not differ ($P > 0.1$). Because $\gamma_o \simeq 0$ when S.L. = 3.0 μ (Figs. 8 and 9), calculation of γ_{i+o} at this extension should give the equivalent tension of R_i, $\gamma_{i+o} - \gamma_o$ (equation 10). The average value of γ_{i+o} was found for each of 17 fibers in Ringer and of 5 fibers in hypotonic Ringer in two intervals of S.L., between 2.75 and 3.0 μ and between 3.0 and 3.25 μ. The mean of the average fiber values in hypotonic Ringer was between 15 and 75% of the mean in Ringer for these two intervals ($P = 0.05$) which shows that hypotonic treatment significantly reduces the tension contribution of R_i. Hypotonic solutions also swell the fibers. Taking nonosmotic fiber volume as 33% (Blinks, 1965), myofibrillar density would be expected to decrease by 15–25% in these

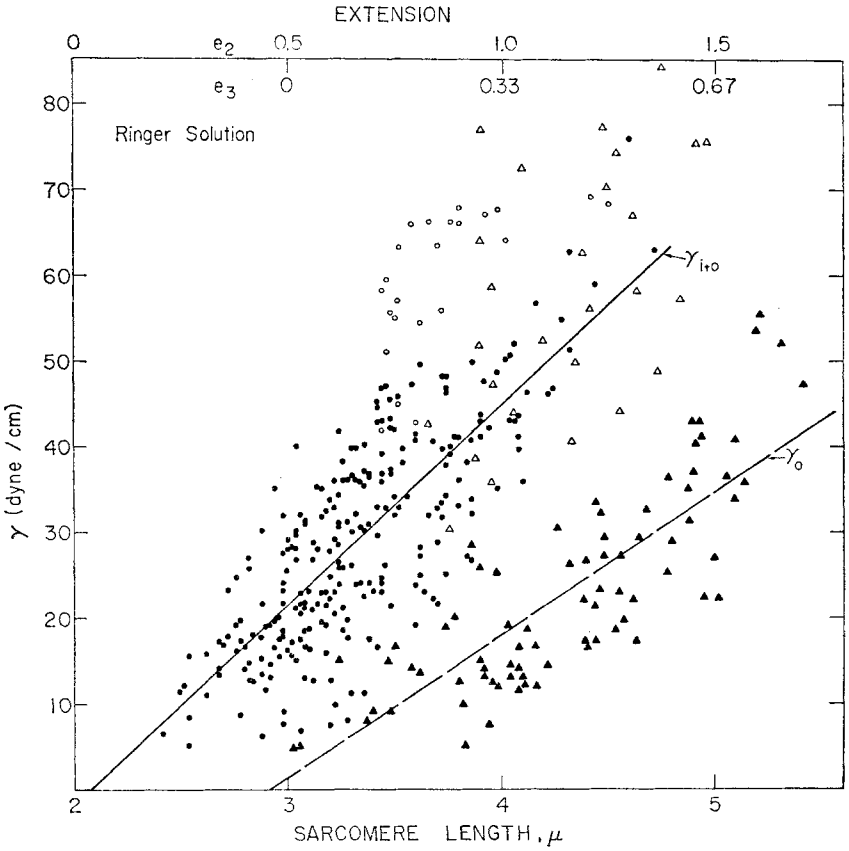

FIGURE 8. Relation of γ_{i+o} and γ_o to sarcomere length and extension. Individual observations are presented. The regression lines are calculated from filled symbols, which represent observations in the elastic regions (see text). Open symbols represent inelastic observations (see text). Circles are for γ_{i+o}, triangles for γ_o. The upper abscissa relates e_2 to e_3. The regression of γ_o against e_3 has a slope of 50.8(95% limits are 42–59) dyne/cm.

solutions, and thus could account for the observed decrease in $\gamma_{i+o} - \gamma_o$ (see Buchthal et al., 1951, p. 95).

Reduction of γ_{i+o} in hypotonic Ringer is reversible. The mean γ_{i+o} of four fibers returned to Ringer after hypotonic treatment was compared with each of the means for Ringer and hypotonic Ringer, in the S.L. interval between 3 and 3.25 μ. γ_{i+o} was significantly greater ($P < 0.02$) in return Ringer than in hypotonic Ringer, but the return value was significantly different from the Ringer value ($P > 0.05$) (Fig. 10).

FORMATION OF CONTRACTURE CLOT Fig. 3 shows that, if pressure is increased beyond 50 dyne/cm^2, the region R_i, which has at first pulled back to

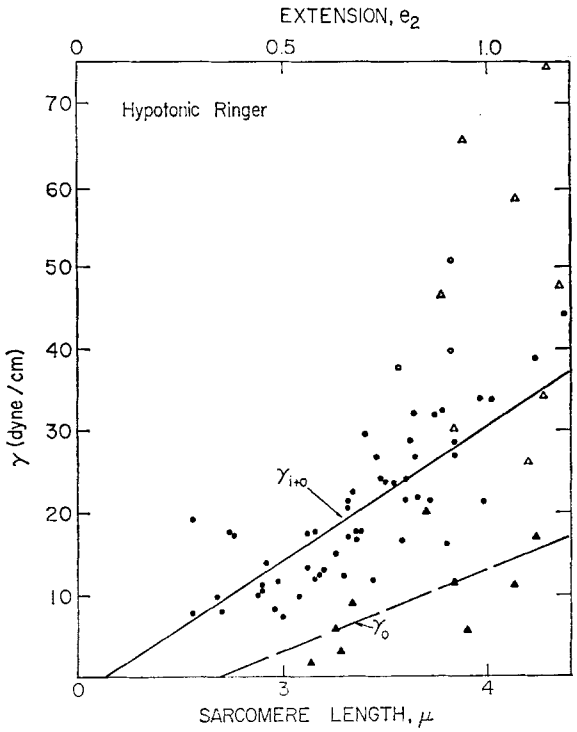

FIGURE 9. Relation of γ_{i+o} and γ_o in hypotonic Ringer to sarcomere length and extension. Individual observations are presented. The regression lines are calculated from filled symbols, which represent observations in the elastic regions. Open symbols represent inelastic observations. Circles are for γ_{i+o}, triangles for γ_o.

the pipette mouth after separating from M_o, bulges out again (Fig. 3 *d*). This should not be interpreted to mean that a significant pressure drop occurs across R_i to stretch it after it has separated from M_o. Inclusion of the factor f in equation 3 shows that R_i is not stretched in Fig. 3 *d*, although it is pulled into the pipette (see Discussion). For Fig. 3 *d*, $f = 1.39$ and $e = 0.03$.

The S.L. in the fiber is reduced by 17% in Fig. 3 *d*, and is also reduced in the upper fiber region of Fig. 3 e. Observations at different periods after that of Fig. 3 *d* show that sarcomere periodic structure disappears in the region R_i and in the fiber adjacent to the pipette mouth. This may indicate a local contracture produced by damage to the surface of R_i. The vertical displacement h of M_o in Fig. 3 *e* is less than that in Fig. 3 *d*, possibly because of this process. A gross contracture does not form until the pipette is separated from the fiber (Fig. 3 *f*). These observations suggest that the plasma membrane covering R_i has been damaged before release but that the pipette seal has provided enough electrical isolation to reduce injury current below that required for a gross contracture.

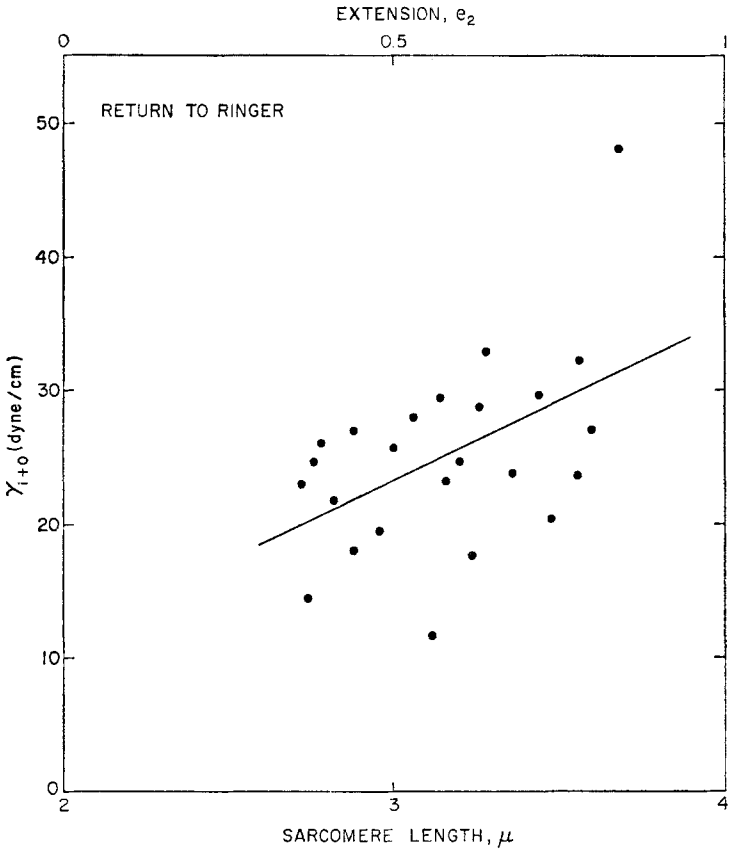

FIGURE 10. Relation of γ_{i+o} to sarcomere length and extension in Ringer after fibers had been soaked at least ½ hr in hypotonic Ringer and returned to Ringer. γ_{i+o} does not differ significantly from its value in Ringer ($P > 0.05$).

At the mouth of the pipette in Fig. 3 *d*, S.L. = 2.0 μ, which is close to the 1.9 μ estimated by Gonzalez-Serratos (1966) as the minimal S.L. of the unstretched fiber. This also demonstrates that bulging is due to an overabundance of sarcomeres because of the attachment of R_i to M_o at the fiber surface.

DISCUSSION

Elastic Modulus of M_o

The intact sarcolemma contains four layers from inside to outside—plasma membrane (100 A thick), basement membrane, collagen layer, and elastic fiber layer (Mauro and Adams, 1961). Electron microscopy indicates that the three outer layers are merged (Reed et al., 1966), and they will separate in vivo from the inner plasma membrane (Birks et al., 1959). Damage to the plasma membrane, or its separation from the fiber, would probably depolarize the

fiber and produce a contracture, because the plasma membrane is continuous with the transverse tubular system (Franzini-Armstrong, 1964).

Since M_o separates from the fiber without causing contracture, and its reference extension and elastic modulus agree with values determined for the sarcolemma by other means (see below), M_o probably is composed of the three outer, merged layers of the sarcolemma. It would have a thickness of about 0.1 μ (Jones and Barer, 1948; Wang, 1956; McCollester, 1962, but see Koketsu et al., 1964).

The elastic modulus of a membrane is defined by the equation (Condon and Odishaw, 1958):

$$E = \gamma/(\text{thickness } x\, e) \tag{11}$$

where e is reference extension and γ is membrane tension. When calculating the modulus of M_o, we ignore the circumferential tension because it is only 15% of the longitudinal component (Rapoport and FitzHugh, 1971). The slope of γ_o against e_3 in Fig. 8 is 50.8 dyne/cm, and substitution into equation 11 for thickness = 0.1 μ gives a value of 5×10^6 dyne/cm^2 for the longitudinal elastic modulus E of the sarcolemma. This value is an upper bound because the equality in equation 8 was used and because circumferential tension was ignored. It is close to the value of $1\text{–}11 \times 10^7$ dyne/cm^2 found by Rapoport and FitzHugh (1971) and Rapoport (unpublished results) for the sarcolemmal tubular preparation. It is less than that found by Fields (1970) for the tubular preparation, perhaps because he worked in the inelastic region of extension. E is larger than the value found for membranes of the egg and other cells, except perhaps at their breaking limits (Hiramoto, 1970).

Division of extension into an elastic region, between S.L. = 3 and ≤ 3.75 μ, and an inelastic region, in which E and γ_o increase (Fig. 8), may arise from complicated structural rearrangements in the multilayered sarcolemma. The sarcolemma contains collagen fibrils whose elastic modulus is 10^{10} dyne/cm^2 (Harkness, 1968). Between S.L. = 3 and 3.75 μ, it can be extended linearly with an elastic modulus about $1/1000$ that of collagen. These observations may mean that elasticity of the sarcolemma at low extensions is due to elastic fibers or to a loose fiber meshwork (see Carton et al., 1962), and that at higher extensions there is a progressive recruitment of slack collagen fibrils, which may or may not have a helical arrangement around the fiber (Fields, 1970; Boyde and Williams, 1968).

Construction of Sarcolemmal Length-Tension Curves from Elastimeter Measurements

A fiber stretches at constant volume (Huxley, 1953). Therefore, fiber diameter d at any sarcomere length can be obtained from d_2 at S.L. = 2 μ:

$$d = d_2 \sqrt{2\,\mu/\text{S.L.}}. \qquad (12)$$

In these experiments, the mean value of d_2 was 95 μ, and was chosen as the reference diameter for calculating comparative length-tension curves of sarcolemma, myoplasm, and whole fiber. The sarcolemmal contribution was obtained by multiplying γ_o by fiber circumference πd, where d was found by equation 12.

Fig. 11 shows calculated length-tension sarcolemmal curves for individual experiments in Ringer and hypotonic Ringer (γ_o was the same in these solutions). These curves in general exhibit two slopes, a gradual one at S.L. = 3–3.75 μ, and a steep one commencing between 3.75 and 4.9 μ. The two slopes correspond to the elastic and inelastic data points of Figs. 8 and 9. The

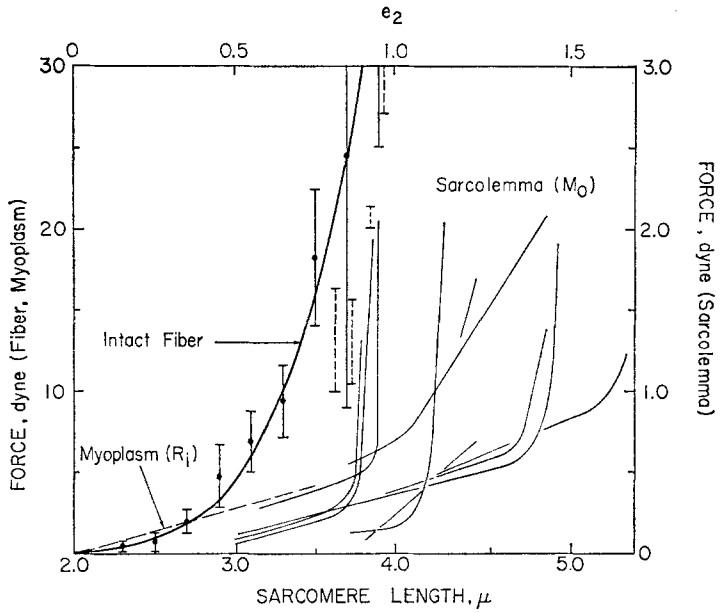

FIGURE 11. Relation of calculated length-tension diagrams of myoplasm (R_i) and of sarcolemma (M_o) to observed length-tension diagram of intact fiber. The standard fiber diameter at S.L. = 2 μ was taken as d_2 = 95 μ, and d was calculated by equation 12. Myoplasmic and fiber tensions per square centimeter can be obtained by dividing force by fiber cross-section, $\pi d^2/4$. The intact fiber curve was fit by eye to mean tensions (±95% limits) found by Rapoport (unpublished results), using the method of Rapoport and FitzHugh (1971). Ranges of intact fiber tensions found by Gordon et al. (1966) are shown as vertical dashed lines, and are close to the intact fiber curve. The myoplasmic length-tension curve was calculated by integrating E, given as a function of e_2 by the regression equation of Fig. 15, between $e_2 = 0$ and e_2, and then by multiplying by $\pi d^2/4$. The sarcolemmal length-tension curves were calculated for individual fibers by multiplying tensions γ_o at a given sarcomere length by fiber circumference, πd. The standard deviations and errors of the observations are discussed in the text with reference to Figs. 8 and 9.

broadness of the length interval where the slope increases may be due to differing amounts of irreversible deformation of M_o. Irreversible changes take place at extensions corresponding to S.L. $\simeq 4.5\ \mu$ (Rapoport and Fitz-Hugh, 1971).

The regression line relating γ_o to S.L. in Fig. 8 shows that $\gamma \simeq 0$ at S.L. $= 3\ \mu$. The sarcolemmal curves in Fig. 11, when compared to the length-tension curve of the intact fiber, also show that the sarcolemma does not contribute to fiber tension at S.L. $\leq 3\ \mu$, contributes 10% or less between 3 and 3.75 μ, and proportionately more beyond 3.75 μ. These higher extensions require high suction pressures which may deform M_o and draw in R_i (e.g. Fig. 3), and may be more appropriately studied with the sarcolemmal tube preparation.

These conclusions agree with those of Casella (1950), who showed that the sarcolemma did not make an important contribution to passive muscle tension. It is uncertain why Podolsky (1964) found more of a contribution at S.L. $\leq 3.75\ \mu$. Perhaps the stripped fiber in oil has altered elastic properties. On the other hand, the sarcolemma of M_o and of the tubular preparation may be abnormal, and the observations are very variable (see below). We do not have enough information to decide between these two alternatives at present.

Elastic Modulus of Myoplasm and Myoplasmic Contribution to Intact Fiber Tension

Equations 7 and 8 can be used to estimate γ_o and therefore the modulus of M_o in a straightforward way because M_o is a thin membrane. Since R_i is a thick myoplasmic region, its elastic modulus cannot be obtained directly from its equivalent tension $\gamma_{i+o} - \gamma_o$ (equation 10). In the Appendix, a model is proposed which ascribes the resistance to deformation by R_i to myoplasmic elasticity rather than to myoplasmic rigidity. Bending rigidity has been used to interpret earlier elastimeter observations on other cells (Mitchison and Swann, 1954; Rand and Burton, 1964).

The model ascribes resistance to deformation by R_i to stretching of uniform longitudinal tension lines within a depth g in the fiber under the pipette cross-section (Fig. 16). These lines correspond to nonuniform myofibrils or filaments, are elastic, and do not resist bending. Fig. 12 shows myofibrillary outlines the distribution of which is like that of the tension lines of Fig. 16; the myofibrils also appear to separate with progressive displacement.

Without assuming a specific distribution of tension lines in the bleb, it is possible by equation 9 a to estimate a lower bound for E. For $h/c \simeq 0.1$ and $g \leq c$ ($c \simeq 30\ \mu$), the data show that $P - \gamma_o/r \simeq 5 \times 10^3$ dyne/cm^2 at S.L. $\simeq 3\ \mu$. Therefore, if the elastic model of the Appendix is correct, $E > 5 \times 10^3$ dyne/cm^2. This minimal value is consistent with other observations (see

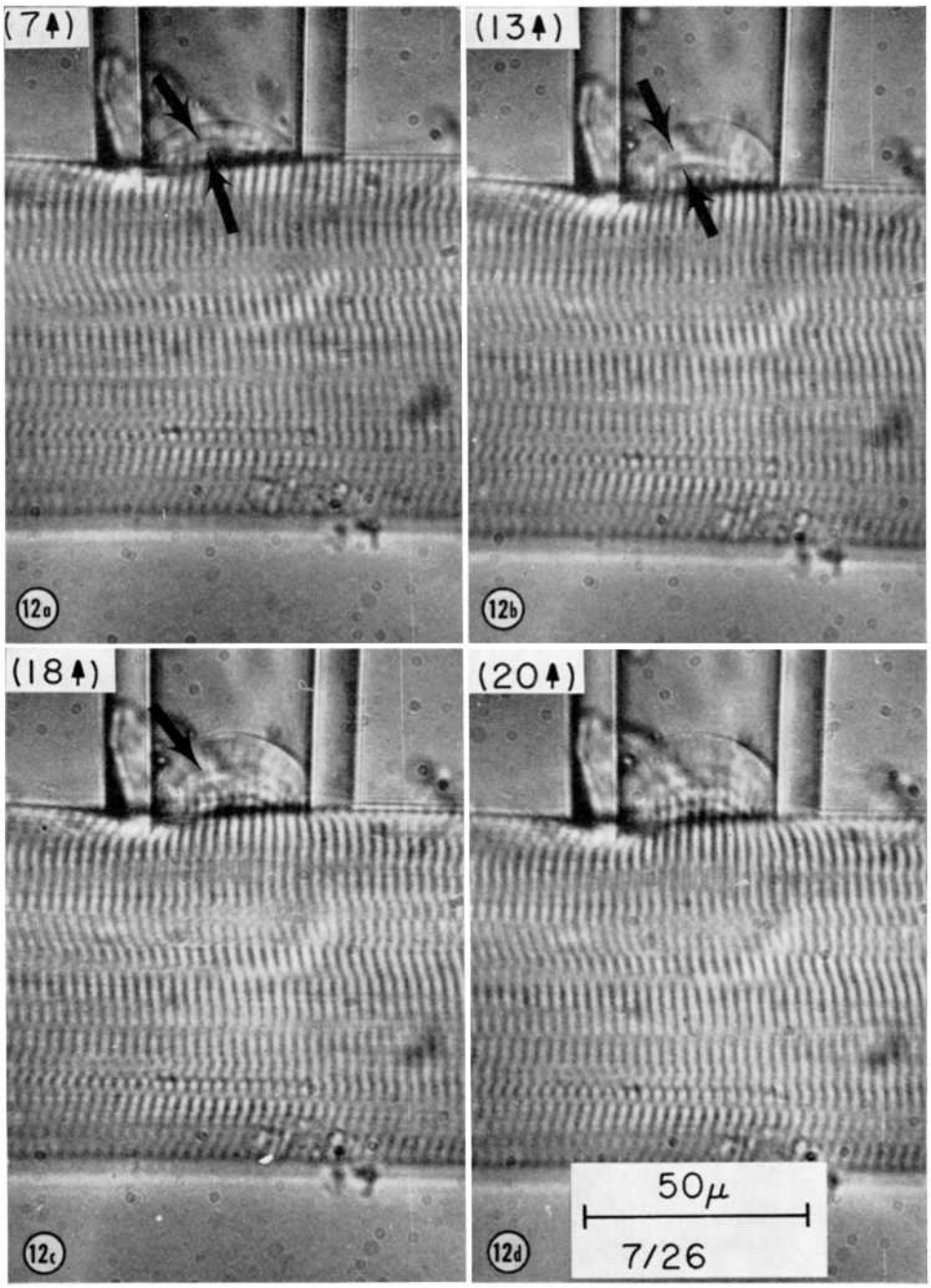

FIGURE 12. Formation of bleb at a fiber region. S.L. = 2.74 μ, 75% hypotonic Ringer. In this series, bleb does not form a spherical arc, but adheres to the sides of the pipette. The distribution of the myofibrils is like the distribution of tension lines in Fig. 16. Arrows point out what appears to be spreading of myofibrils with increasing displacement.

below), and supports the interpretation that resistance to deformation by R_i is due to myoplasmic elasticity.

An accurate estimate of E is not afforded by the model at present because of three unknowns, the depth g to which tension lines in the bleb are displaced, the distribution of tension lines within the bleb, and the inequality relation of equation 8. For these reasons, the value of myoplasmic E estimated below should be considered to be only approximate.

If tension line density is constant in the bleb (equation 12 *a*, $\alpha = 1$ in equation 10 *a*), equation 13 *a* predicts that a plot of $P - \gamma_o/r$ against $\ln(1 + 4h^2/c^2)$ at $h \simeq 0$ should have a constant slope equal to Ee_2g/h, if g/h remains constant. Figs. 13 and 14 demonstrate this initial slope. Furthermore, a plot of $P - \gamma_o/r$ against h/c, found in most of the experiments to reach an asymptote as in Fig. 13, can be interpreted to mean that the ratio g/h decreases with vertical displacement. This is probable because initially $h \simeq 0$; furthermore, the maximal limit of g is the diameter d of the fiber, where $d \geq 2c$. If tension line density decreased as a linear function of y (Fig. 17, $\alpha =$

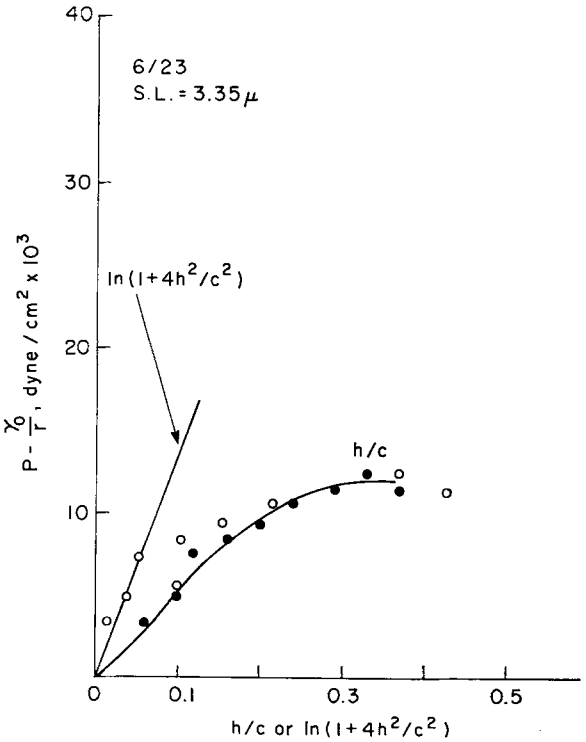

FIGURE 13. Relation of $(P - \gamma_o/r)$, the pressure contribution of region R_i, to functions of bleb displacement, h/c and $\ln(1 + 4h^2/c^2)$. The factor f is included in the calculations. The initial slope against $\ln(1 + 4h^2/c^2)$ is 1.20 dyne/cm^2 $\times$ 10^5; by equation 13 *a*, $E = 1.77 \times 10^5$ dyne/cm^2. The curve with h/c as the abscissa was fit by eye.

2 in equation 10 *a*), the observed asymptotes still show that g/h decreases with vertical displacement of the bleb.

Values of E obtained from the initial slopes for constant tension line density at $g/h = 1$ are plotted against sarcomere length and e_2 in Fig. 15. The regression line in the figure predicts a myoplasmic resting tension at S.L. = 2.1 μ ($e_2 = 0.05$) of 4×10^3 dyne/cm^2, which is found by Hill (1968) as the fila-

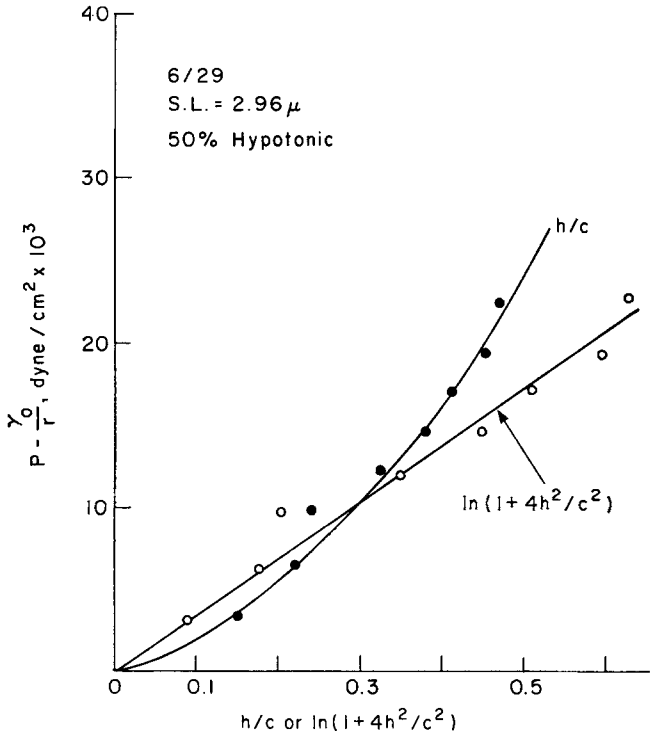

FIGURE 14. Relation of $(P - \gamma_o/r)$ to h/c and to $\ln(1 + 4h^2/c^2)$. The factor f is included in the calculations. The initial slope against $\ln(1 + 4h^2/c^2)$ is 0.344×10^5 dyne/cm^2; by equation 13 *a*, $E = 0.72 \times 10^5$ dyne/cm^2. The curve for h/c as the abscissa was fit by eye.

mentary resting tension at this extension. This suggests that the estimates of E are reasonable. If line density decreased with displacement x ($\alpha > 1$ in equation 10 *a*), the E's in Fig. 15 would be overestimates.

The myoplasmic length-tension curve, as calculated from the line in Fig. 15 for $d_2 = 95$ μ, agrees roughly with the length-tension curve of the intact fiber at S.L. < 3.5 μ, as shown in Fig. 11. This further supports the estimates of E by use of the elasticity model of the Appendix.

Since myoplasmic elasticity does not appear to decrease when there is little or no overlap of the actin and myosin filaments (at or above S.L. =

3.6 μ; Huxley, 1964), it may not be due to interfilamentary interaction as suggested by Hill (1968). It may arise from electrostatic interactions between filaments (Elliott, 1967; Shear, 1969) or from other elastic properties of the myoplasm.

Assumptions and Methods

It is not certain how closely suction pressure P approximates the pressure drop across M_o when M_o has separated from R_i (see assumption [b] and equation 8). The factor f was used in equation 3 to calculate the extra surface of R_i drawn

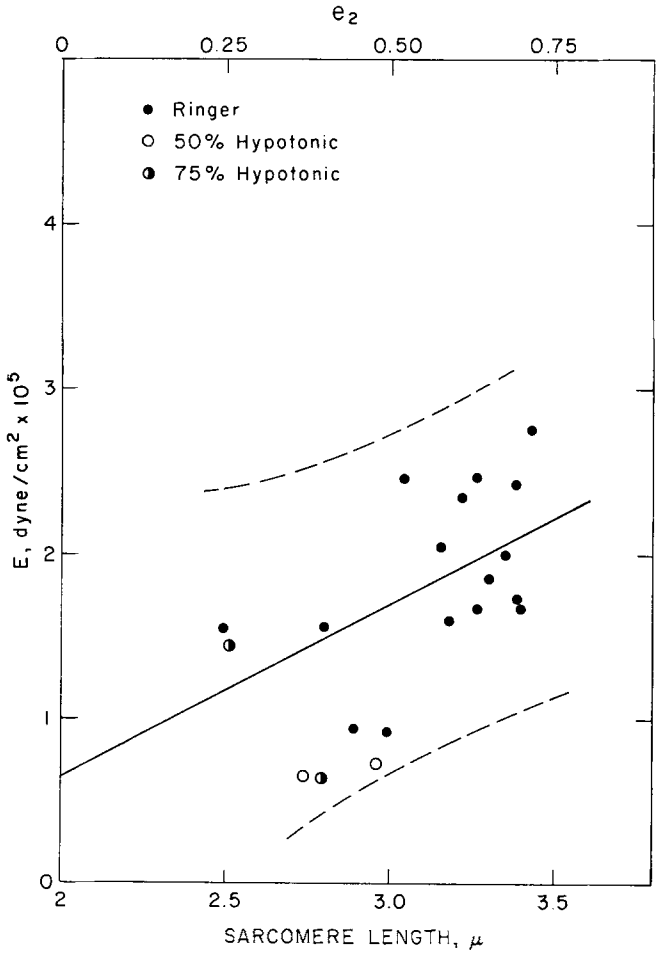

FIGURE 15. Relation of myoplasmic elastic modulus E, as calculated by the model in the Appendix, to sarcomere length and extension, e_2. The regression line is given as $E = (0.66 + [2.06]e_2) \times 10^5$ dyne/cm^2.The slope was significantly > 0 ($P < 0.05$), and the 95 percentile limits are shown in the figure. Ringer observations only were used to calculate the line and its limits.

into the pipette and to refer extension e to the initial + extra surface. f may be >1 if bulging of R_i comes from its being pulled into the pipette by M_o, since R_i is attached to M_o at the pipette circumference (Figs. 2 and 3). f could be >1 also if a significant pressure drop across R_i pulled it directly into the pipette. In the latter case, e would be >0, since R_i is extensible. Since $e \simeq 0$ for $P < 50$ dyne/cm^2, bulging of R_i must be due mainly to its attachment to M_o, and the pressure drop across M_o is probably close to suction pressure.

Water flow across M_o and R_i must occur at all pressures (Blinks, 1965), but it is not enough to displace fat droplets in the connecting capillary of Fig. 1 *a*. Separation of M_o from R_i might be facilitated by water flow between these regions from the muscle or from the exterior fluid because of the absence of a tight seal.

At S.L. = 4 μ, Fig. 8 shows that $\gamma_{\text{circumferential},o} \simeq 3$ dyne/cm, assuming $\gamma_{\text{circumferential},o}$ is 15% of $\gamma_{\text{longitudinal},o}$ (Rapoport and FitzHugh, 1971). For a fiber of radius = 47 μ, equation 6 shows that the internal pressure due to circumferential tension is about 1×10^3 dyne/cm^2 ($r_2 = \infty$ for a cylinder). Suction pressure is usually greater by a factor of 10 or more, so that internal hydrostatic pressure can be neglected (see Rand and Burton, 1964). Similar conclusions apply at all S.L.'s.

The questions of deformation of M_o and of its composition cannot be resolved without electron microscopy. Reasons to consider M_o to contain the three outer sarcolemmal layers were presented. The fiber is not damaged when M_o is separated. The reference extension of M_o agrees with that found indirectly by Podolsky (1964), and its elastic modulus is the same as for the tubular sarcolemma, which contains intact the three outer sarcolemmal layers (Mauro and Adams, 1961). These facts suggest that major changes in M_o or in the fiber have not been produced by the elastimeter method.

The variability of the results (Fig. 11) may be due to different quantities of connective tissue in the bleb region, or to slight leaks at the pipette mouth which were not picked up by the fat droplet observations (Methods). Use of the factor f permits distinguishing stretch of original membrane from indrawing of new membrane into the pipette. This distinction does not obtain when the elastimeter method is applied to other tissues.

APPENDIX

Elastic Model of R_i

ASSUMPTIONS (a_1) Let myoplasmic tension be due to a continuous array of longitudinally oriented and uniform tension lines. The elastic modulus is the modulus of each line times the number of lines per square centimeter of the cross-section. Let line tension be proportional to extension.

(b_1) For a bleb of vertical displacement h (Fig. 16), let lines to a depth g in the body of the fiber be displaced upward by a distance $x(y)$ to a maximum displacement $x = h$ at $y = g + h$. Also, $x = 0$ at $y = 0$.

(c_1) Let resistance to deformation by the bleb arise from summative elastic effects of line tension to a depth g and be independent of line rigidity or bending. Circumferential elasticity, representing lateral interaction between adjacent tension lines, is much less than longitudinal elasticity (Sten-Knudsen, 1953), and can be ignored.

DERIVATION At the fiber S.L. at which the bleb is formed, resting myoplasmic tension is Ee_2, where E is the myoplasmic elastic modulus in the fiber body and e_2 the extension referred to S.L. $= 2\mu$ (equation 5). When the surface of the bleb or of a tension line is extended beyond e_2 by an increment e (equation 3), e_2 is increased by Δe_2, obtained from equations 3 and 5 for $f = 1$:

$$\Delta e_2 = e(\text{S.L.}/2\mu). \tag{1 a}$$

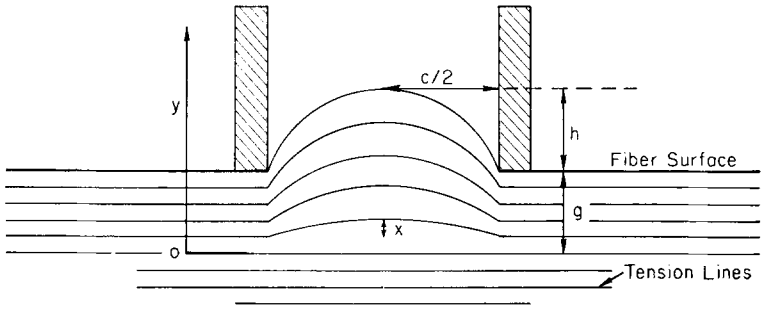

FIGURE 16. Diagram of assumed distribution of tension lines in region R_i of bleb and below it to depth g. The longitudinal lines are uniform tension lines with a continuous density in the y direction. The plane shown in the figure passes through the fiber axis and the diameter of the pipette mouth. x is the vertical displacement of any tension line to a maximum value of $x = h$. Pipette diameter $= c$. $y = 0$ at depth g.

Δe_2 as a function of vertical displacement x is obtained by the use of equations 3 and 1 a for tension lines in the plane passing through both the longitudinal fiber axis and the diameter c of the pipette mouth (Fig. 16). Interaction with tension lines in adjacent planes can be ignored according to assumption (c_1).

$$\Delta e_2(x) = \left(\frac{\text{S.L.}}{2\mu}\right)\left(\frac{s(x) - c}{c}\right). \tag{2 a}$$

The stretch $s(x)$ of a tension line whose vertical displacement is x is given by (see equation 4, Fig. 5 a)

$$s(x) = 2r(x)\sin^{-1}(c/2r[x]) \tag{3 a}$$

where $r(x)$ is the radius of curvature of the displaced line (see equation 1).

$$r(x) = c^2/8x + x/2. \tag{4 a}$$

A tension line initially at y_o is displaced to $y = y_o + x(y_o)$ in the bleb. Differentiating

y with respect to y_o and rearranging gives

$$dy = \left(\frac{1}{1 - dx/dy}\right) dy_o . \tag{5 a}$$

The initial number of tension lines in thickness dy_o equals the number of lines in corresponding thickness dy in the bleb, where $dy_o \leq dy$. The ratio of tension line density in the bleb to density before bleb formation is dy_o/dy. We define an elastic modulus $E(y)$ as a monotonic function of y for $y \geq 0$ in the bleb, letting $E(y)$ at $y = 0$ equal E. By assumption (a_1), $E(y)$ is proportional to line density at y, and equals $E(dy_o/dy)$. By equation 5 a,

$$E(y) = E(1 - dx/dy). \tag{6 a}$$

The pressure due to R_i is given by equation 10 as the difference between the suction pressure applied to the whole bleb and the contribution of M_o, or $P - \gamma_o/r$. By the Laplace equation (see equation 6 and Hooke's law), the pressure contribution of each line is

$$[\text{elastic line modulus}] \cdot \frac{[e_2 + \Delta e_2(x)]}{r(x)} . \tag{7 a}$$

Integrating the contribution from all lines between $y = 0$ and $y = g + h$ gives

$$P - \gamma_o/r = \int_o^{g+h} \frac{E(y)[e_2 + \Delta e_2(x)]}{r(x)} dy . \tag{8 a}$$

Before obtaining specific solutions for E, we will calculate its lower bound. By equation 4 a, $1/r(x) < 8h/c^2$. Also $E(y) \leq E$, as defined above. Finally, $e_2 + \Delta e_2 \leq [\pi(\text{S.L.})/4\,\mu - 1]$, by definition. Inserting these inequalities into equation 8 a, and then integrating, gives a lower bound for E,

$$E > \frac{(P - \gamma_o/r)c^2}{8h(g + h)[\pi(\text{S.L.})/4\,\mu - 1]} . \tag{9 a}$$

Calculation of the myoplasmic modulus depends on two unknown factors: (a) g as a function of h and (b) the distribution of displaced tension lines between $y = 0$ and $y = g + h$. This distribution can be obtained from the relation between x and y. One set of equations consistent with assumption (b_1) is of the form

$$x = \frac{h}{(g + h)^\alpha}\, y^\alpha . \tag{10 a}$$

The maximum depth in which the tension lines can be displaced is the diameter d of the fiber, so that $0 \leq g \leq d$.

Substituting equation 6 a in equation 8 a, and changing the variable of integra-

tion from y to x by equation 10 a, yields the following:

$$P - \gamma_o/r = E\int_o^h \left[\frac{(g+h)x^{(1/\alpha-1)}}{\alpha h^{1/\alpha}} - 1\right]\left[\frac{e_2 + \Delta e_2(x)}{r(x)}\right] dx\,. \qquad (11\ a)$$

The expressions for $r(x)$, $\Delta e_2(x)$, and $s(x)$ are given above. For a positive integer α, by use of the mean value theorem of integral calculus, it can be shown that $P - \gamma_o/r$ will be a monotonically increasing function of h/c if the ratio g/h remains constant.

Specific solutions for E can be obtained with equation 10 a by choosing different values of α. When $\alpha = 1$, $E(y)$ is constant and x is a linear function of y

$$E(y) = Eg/(g+h) \qquad x = hy/(g+h). \qquad (12\ a)$$

Using a series expansion for $\sin^{-1}(c/2r[x])$, equation 10 a gives

$$(P - \gamma_o/r) = (gE/h)[e_2 \ln(1 + 4h^2/c^2) + \frac{\text{S.L.}}{c}\int_o^h \left[(1/6)\left(\frac{cx}{c^2/4 + x^2}\right)^3 + (3/40)\left(\frac{cx}{c^2/4 + x^2}\right)^5 \cdots\right] dx]\,. \qquad (13\ a)$$

The integral term was solved by computer. The continuous curves of Fig. 17 are

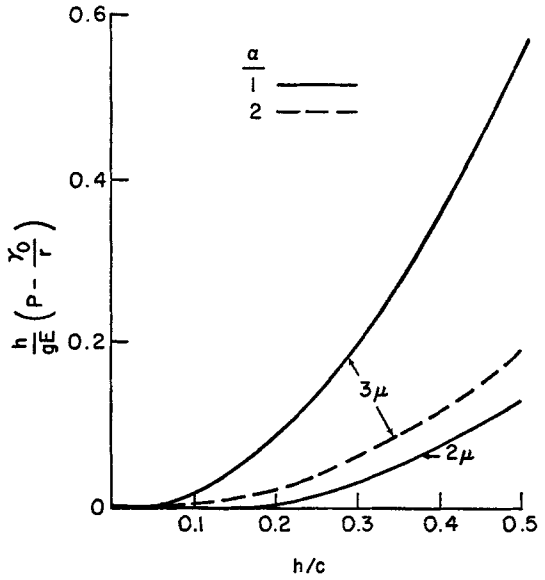

FIGURE 17. Plots of $(h/gE)\ (P - \gamma_o/r)$ against h/c as calculated by equation 13 a, for different sarcomere lengths and tension line distributions. The continuous curves at S.L. = 3 and 2 μ are calculated for g/h a constant, when x increases linearly with y (Fig. 16), and when line density and $E(y)$ are constant (equation 12 a). The dashed curve at S.L. = 3 μ is calculated for $h/g = 1$, when x increases with y^2, and when line density and $E(y)$ decrease linearly with y (equation 14 a).

plots of $(h/gE)(P - \gamma_o/r)$ against h/c for initial S.L. = 3 and 2 μ. If g/h is constant, the ordinate at S.L. = 3 μ increases steeply. If g/h decreases with increasing h, the curve can flatten out.

For $h/c \simeq 0$, the integral in equation 13 a is much smaller than the logarithmic contribution. For g/h constant, a plot of $(P - \gamma_o/r)$ against $\ln(1 + 4h^2/c^2)$ should be linear initially at S.L. = 3 $\mu(e_2 \gg 0)$, with a slope equal to $Ee_2(g/h)$ (see Figs. 13 and 14).

While a value of $\alpha = 1$ implies a constant line density and elastic modulus for $y > 0$, if $\alpha = 2$ line density and modulus decrease linearly with y and displacement x increases as y^2:

$$E(y) = E\left(1 - \frac{2hy}{(g + h)^2}\right) \qquad x = \frac{hy^2}{(g + h)^2}. \tag{14 a}$$

The interrupted curve of Fig. 17 shows the relation of $(P - \gamma_o/r)/E$ to h/c at S.L. = 3 μ. g/h was taken as 1. This curve increases monotonically as predicted above and would become asymptotic only if the ratio g/h decreased with increasing h. As α increases, the curves for $\alpha > 2$ will be closer to the h/c axis.

I thank Mr. Rufus Gunn for his very valuable technical assistance, and Doctors Clifford Patlak, Richard FitzHugh, and Harold Lecar for their helpful discussions. Mrs. Karen Pettigrew, Section on Theoretical Statistics and Mathematics, National Institute of Mental Health, aided with the statistical analysis of the data.

Received for publication 30 August 1971.

REFERENCES

BIRKS, R., B. KATZ, and R. MILEDI. 1959. Dissociation of the surface membrane complex in atrophic muscle fibers. *Nature (London).* **184**:1507.

BLINKS, J. R. 1965. Influence of osmotic strength on cross-section and volume of isolated single muscle fibers. *J. Physiol. (London).* **177**:42.

BOYDE, A., and J. C. P. WILLIAMS. 1968. Surface morphology of frog striated muscle as prepared for and examined in the scanning electron microscope. *J. Physiol. (London).* **197**:10P.

BROWNLEE, K. A. 1965. Statistical Theory and Methodology in Science and Engineering. John Wiley and Sons Inc., New York. 2nd edition.

BUCHTHAL, F., E. KAISER, and P. ROSENFALCK. 1951. The rheology of the cross striated muscle fibre. *Dan. Biol. Medd.* **21**:1.

CARTON, R. W., J. DAINAUSKAS, and J. W. CLARK. 1962. Elastic properties of single elastic fibers. *J. Appl. Physiol.* **17**:547.

CASELLA, C. 1950. Tensile force in total striated muscle, isolated fibre and sarcolemma. *Acta Physiol. Scand.* **21**:380.

CONDON, E. U., and H. ODISHAW. 1958. Handbook of Physics. McGraw-Hill Book Company, New York. **3**:67.

DULL, R. W. 1941. Mathematics for Engineers. McGraw-Hill Book Company, New York. 2nd edition.

ELLIOTT, G. F. 1967. Variations of the contractile apparatus in smooth and striated muscles. *J. Gen. Physiol.* **50**(6, Pt. 2):171.

FATT, P. 1964. An analysis of the transverse electrical impedance of striated muscle. *Proc. Roy. Soc. Ser. B Biol. Sci.* **159**:606.

FIELDS, R. W. 1970. Mechanical properties of the frog sarcolemma. *Biophys. J.* **10**:462.

FONBRUNE, P. DE. 1949. Technique de Micromanipulation. Massoon et Cie, Paris.

FRANZINI-ARMSTRONG, C. 1964. Fine structure of sarcoplasmic reticulum and transverse tubular system in muscle fibers. *Fed. Proc.* **23**:887.

GONZALEZ-SERRATOS, H. 1966. Inward spread of contraction during a twitch. *J. Physiol. (London).* **185**:20P.

GORDON, A. M., A. F. HUXLEY, and F. J. JULIAN. 1966. Tension development in highly stretched vertebrate muscle fibres. *J. Physiol. (London).* **184**:143.

HARKNESS, R. D. 1968. *In* Treatise on Collagen. B. S. Gould, editor. Academic Press, Inc., New York. **2**(A).

HILL, D. K. 1968. Tension due to interaction between sliding filaments in resting striated muscle. *J. Physiol. (London).* **199**:637.

HIRAMOTO, Y. 1970. Rheological properties of sea urchin eggs. *Biorheology.* **6**:201.

HUXLEY, A. F. 1964. Muscle. *Annu. Rev. Physiol.* **26**:131.

HUXLEY, H. E. 1953. X-ray analysis and the problem of muscle. *Proc. Roy. Soc. Ser. B Biol. Sci.* **141**:59.

JONES, W. M., and R. BARER. 1948. Electron microscopy of the sarcolemma. *Nature (London).* **161**:1012.

JOOS, G. 1958. Theoretical Physics. Blackie and Son Ltd., London. 3rd edition.

KOKETSU, K., R. KITAMURA, and R. TANAKA. 1964. Binding of calcium ions to cell membrane isolated from bullfrog skeletal muscle. *Amer. J. Physiol.* **207**:509.

MAURO, A., and W. R. ADAMS. 1961. The structure of the sarcolemma of the frog skeletal muscle fiber. *J. Biophys. Biochem. Cytol.* **10**(4):177.

MCCOLLESTER, D. L. 1962. A method for isolating skeletal muscle cell membrane components. *Biochim. Biophys. Acta.* **57**:427.

MITCHISON, J. M., and M. M. SWANN. 1954. The mechanical properties of the cell surface. *J. Exp. Biol.* **31**:443.

PODOLSKY, R. J. 1964. The maximum sarcomere length for contraction of isolated myofibrils. *J. Physiol. (London).* **170**:110.

RAND, R. P., and A. C. BURTON. 1964. Mechanical properties of the red cell membrane. *Biophys. J.* **4**:115.

RAPOPORT, S. I. 1970. Elasticity of sarcolemma and myoplasm of frog muscle. *Biophys. Soc. 14th Annu. Meet. Abstr.* 217a.

RAPOPORT, S. I., and R. FITZHUGH. 1971. Anisotropic elastic properties of frog muscle sarcolemma in the region of reversible extension. *Biophys. Soc. 15th Annu. Meet. Abstr.* 200a.

REED, R., T. W. HOUSTON, and P. M. TODD. 1966. Structure and function of the sarcolemma of skeletal muscle. *Nature (London).* **211**:534.

SHEAR, D. B. 1969. The electrical double layer, long range forces, and muscle contraction. *Physiol. Chem. Phys.* **1**:495.

STEN-KNUDSEN, O. 1953. Torsional elasticity of the isolated cross striated muscle fibre. *Acta Physiol. Scand. Suppl.* **104**:1.

STREET, S. F., and R. W. RAMSEY. 1965. Sarcolemma: transmitter of active tension in frog skeletal muscle. *Science (Washington).* **149**:1379.

WANG, H. 1956. The sarcolemma and fibrous envelope of striated muscles in beef. *Exp. Cell Res.* **11**:452.